ORIGINAL ARTICLE

JBMR

Assessment of Cortical Interruptions in the Finger Joints of Patients With Rheumatoid Arthritis Using HR-pQCT, Radiography, and MRI

Michiel Peters,[1,2,3] Astrid van Tubergen,[1,2] Andrea Scharmga,[1,2,3] Annemariek Driessen,[2,3,4] Bert van Rietbergen,[5,6] Daan Loeffen,[7] Rene Weijers,[7] Piet Geusens,[1,2,8] and Joop van den Bergh[1,3,8,9]

[1]Department of Internal Medicine, Division of Rheumatology, Maastricht University Medical Center, Maastricht, The Netherlands
[2]Research School CAPHRI, School for Public Health and Primary Care, Maastricht, The Netherlands
[3]NUTRIM School of Nutrition and Translational Research in Metabolism, Maastricht University, Maastricht, The Netherlands
[4]Department of Clinical Pharmacy and Toxicology, Maastricht University Medical Center, Maastricht, The Netherlands
[5]Faculty of Biomedical Engineering, Eindhoven University of Technology, Eindhoven, The Netherlands
[6]Department of Orthopaedic Surgery, Maastricht University Medical Center, Maastricht, The Netherlands
[7]Department of Radiology, Maastricht University Medical Center, Maastricht, The Netherlands
[8]Faculty of Medicine and Life Sciences, Hasselt University, Belgium
[9]Department of Internal Medicine, VieCuri Medical Center, Venlo, The Netherlands

ABSTRACT

Small cortical interruptions may be the first sign of an erosion, and more interruptions can be found in patients with rheumatoid arthritis (RA) compared with healthy subjects. First, we compared the number and size of interruptions in patients with RA with healthy subjects using high-resolution peripheral quantitative CT (HR-pQCT). Second, we investigated the association between structural damage and inflammatory markers on conventional radiography (CR) and MRI with interruptions on HR-pQCT. Third, the added value of HR-pQCT over CR and MRI was investigated. The finger joints of 39 patients with RA and 38 healthy subjects were examined through CR, MRI, and HR-pQCT. CRs were scored using the Sharp/Van der Heijde method. MRI images were analyzed for the presence of erosions, bone marrow edema, and synovitis. HR-pQCT images were analyzed for the number, surface area, and volume of interruptions using a semiautomated algorithm. Descriptives were calculated and associations were tested using generalized estimating equations. Significantly more interruptions and both a larger surface area and the volume of interruptions were detected in the metacarpophalangeal joints of patients with RA compared with healthy subjects (median, 2.0, 1.42 mm^2, and 0.48 mm^3 versus 1.0, 0.69 mm^2, and 0.23 mm^3, respectively; all $p < 0.01$). Findings on CR and MRI were significantly associated with more and larger interruptions on HR-pQCT (prevalence ratios [PRs] ranging from 1.03 to 7.74; all $p < 0.01$) in all subjects, and were consistent in patients with RA alone. Having RA was significantly associated with more and larger interruptions on HR-pQCT (PRs, 2.33 to 5.39; all $p < 0.01$), also after adjustment for findings on CR or MRI. More and larger cortical interruptions were found in the finger joints of patients with RA versus healthy subjects, also after adjustment for findings on CR or MRI, implying that HR-pQCT imaging may be of value in addition to CR and MRI for the evaluation of structural damage in patients with RA. © 2018 The Authors. *Journal of Bone and Mineral Research* Published by Wiley Periodicals Inc.

KEY WORDS: CORTICAL INTERRUPTIONS; RHEUMATOID ARTHRITIS; HIGH-RESOLUTION PERIPHERAL QUANTITATIVE COMPUTED TOMOGRAPHY; BONE MICROARCHITECTURE; RADIOGRAPHY; MAGNETIC RESONANCE IMAGING

Introduction

Rheumatoid arthritis (RA) is a chronic inflammatory autoimmune disease, in which inflammation at the joint may lead to periarticular osteoporosis and erosions (ie, pathological cortical interruptions).[1,2] Traditionally, the presence of erosions is assessed by conventional radiography (CR) in the joints of the hands and feet. However, CR is limited by its sensitivity in the detection of erosions, which is low compared with CT and MRI.[3–6] With CT as a reference method, sensitivity to detect erosions in metacarpophalangeal (MCP) joints was 26% and 68% for CR and MRI, respectively.[7] In addition, MRI is able to visualize

This is an open access article under the terms of the Creative Commons Attribution License, which permits use, distribution and reproduction in any medium, provided the original work is properly cited.
Received in original form December 3, 2017; revised form April 5, 2018; accepted April 29, 2018. Accepted manuscript online May 11, 2018.
Address correspondence to: M. Peters, Department of Internal Medicine, Division of Rheumatology, Maastricht University Medical Center, P.O. Box 5800, NL-6202 AZ Maastricht, The Netherlands. E-mail: michiel.peters@maastrichtuniversity.nl
Additional Supporting Information may be found in the online version of this article.
Journal of Bone and Mineral Research, Vol. 33, No. 9, September 2018, pp 1676–1685
DOI: 10.1002/jbmr.3466
© 2018 The Authors. *Journal of Bone and Mineral Research* Published by Wiley Periodicals Inc.

inflammation in the joint, such as bone marrow edema (BME) and synovitis, which are associated with the progression of bone damage on CR in patients with RA.[8–10]

Another imaging modality used in RA is high-resolution peripheral quantitative CT (HR-pQCT), which can visualize the 3D bone structure of the peripheral skeleton at the microscale level (82-μm isotropic voxel size) in vivo. Comparative studies have shown that HR-pQCT imaging is more sensitive than MRI and CR in the detection of pathological interruptions (ie, erosions) in finger joints.[11–13] In addition, HR-pQCT imaging can evaluate the cortical and trabecular volumetric bone mineral density (vBMD) and bone microstructure in finger joints.[14]

Previous studies that compared patients with RA with healthy subjects using HR-pQCT primarily focused on the visual detection of pathological interruptions.[14–20] In a prior study, we demonstrated that with HR-pQCT a variety of cortical interruptions can be seen in the finger joints of both patients with RA and healthy subjects. Some (larger) cortical interruptions had underlying trabecular bone voids and were suggestive of an erosion, whereas other cortical interruptions were smaller and may represent physiological interruptions (ie, vascular channels).[21] The detection of these smaller interruptions might be of clinical relevance because it has been hypothesized that vascular channels may serve as a starting point for pathological cortical interruptions as the vascular channel provides direct entry for osteoclast-mediated joint destruction.[1,22,23] It has also been shown that the number of visually detected small cortical interruptions is increased in patients with RA compared with healthy subjects.[24] Moreover, the number of visually detected interruptions was increased in patients with a more active disease, suggesting a link to synovitis.[11] Besides the detection of more and larger cortical interruptions in RA, an impaired vBMD and microstructure can be found in the finger joints of patients with RA versus healthy subjects.[14] These parameters at the MCP joints are strongly correlated with the parameters at the distal radius, which are impaired in patients with osteoporosis.[25,26]

Major drawbacks to the visual detection of cortical interruptions are that it is prone to subjectivity and is also time-consuming.[27] In a previous study, we showed that the interoperator reliability of visually detecting these small cortical interruptions was fair.[28] Therefore, we developed and validated a semiautomated algorithm that more reliably detects the number, surface area, and volume of (small) cortical interruptions (diameter $\geq$0.41 mm) in comparison with visual scoring.[28–31]

Although these earlier studies demonstrated the feasibility, validity, and reliability of our semiautomated algorithm in quantifying (small) cortical interruptions, it remains unknown if these (small) cortical interruptions are more frequently seen in patients with RA compared with controls, and whether they are related to both structural damage on CR and structural damage and inflammatory markers on MRI. Furthermore, it is unknown if HR-pQCT imaging has an added value over findings on CR and MRI in the detection of (small) cortical interruptions and in the distinction between patients with RA and healthy subjects.

First, we evaluated the number, surface area, and volume of cortical interruptions (further described as "cortical interruption parameters") detected on HR-pQCT images with our semiautomated algorithm in patients with RA (dominant versus nondominant hand, and early versus longstanding RA patients) and compared our results with healthy subjects. Second, we investigated whether an association exists between structural damage on CR or structural and inflammatory markers on MRI, with the cortical interruption parameters on HR-pQCT in all subjects and in patients with RA alone. Third, we investigated the added value of HR-pQCT in the detection of cortical interruptions and in the distinction between patients with RA and healthy subjects over findings on CR and MRI. Last, we investigated the bone density and microstructure parameters in all subjects and in patients with RA alone, and their association with the cortical interruption parameters.

Materials and Methods

Subjects

For this cross-sectional study, we used data from the MOSA-Hand cohort, which consists of 38 healthy women and 41 female patients diagnosed with RA.[21] All subjects were recruited at the Maastricht University Medical Center, The Netherlands. All patients with RA fulfilled the 2010 American College of Rheumatology (ACR)/European League Against Rheumatism (EULAR) classification criteria for RA.[32] Information on disease duration, medication use, smoking status, anti-citrullinated protein antibody (ACPA), and rheumatoid factor (RF) positivity was retrieved from patients' medical files. Healthy subjects, matched on age by decade, did not suffer from hand-joint complaints. All subjects signed informed consent. Ethical approval was obtained from the ethics board of the academic hospital Maastricht/Maastricht University, The Netherlands (Netherlands Trial Registry number: NTR3821).

HR-pQCT image acquisition

The second and third MCP and proximal interphalangeal (PIP) joints were scanned with HR-pQCT (XtremeCT1, Scanco Medical AG, Switzerland). In healthy subjects only, the dominant hand was scanned; in patients with RA, both hands were scanned. Each hand was separately scanned using a carbon cast for finger scanning as provided by the manufacturer.

For the first 13 subjects (8 healthy subjects and 5 patients with RA) that were scanned, a scan protocol of two stacks was used for MCP joints and one stack for PIP joints (Fig. 1*A*, scan protocol 1). This scan length was in subsequent subjects enlarged to three stacks for MCP joints and two stacks for PIP joints, based on the acquired experience of the Study grouP for xtrEmeCT in RA (SPECTRA; Fig. 1*B*, scan protocol 2).[33] With both scan protocols, the reference line of MCP scans was placed at the top of the second or third metacarpal head (whichever was most distal of the two), and for PIP scans at the second or third proximal interphalange (whichever was most distal of the two). In this way, similar regions of interest were selected and measured. Figure 1 shows that both scan protocols encapsulate the whole joint region, including the total region where cortical interruptions may occur. Therefore, all scans were used for the quantification of cortical interruptions. However, for the bone density and microstructure parameters, the scans of protocol 1 were excluded because a difference in scan length substantially influenced these parameters (Fig. 2).

Scanning was performed at clinical in vivo settings: tube voltage = 60 kVp, tube current = 900 μA, integration = 100 ms. Time and images were reconstructed using an 82-μm isotropic voxel size. Subject scans were evaluated on motion artifacts according to Pialat and colleagues[34] Scans with at least one stack of poor quality (grade >3) were excluded from further analyses.[34]

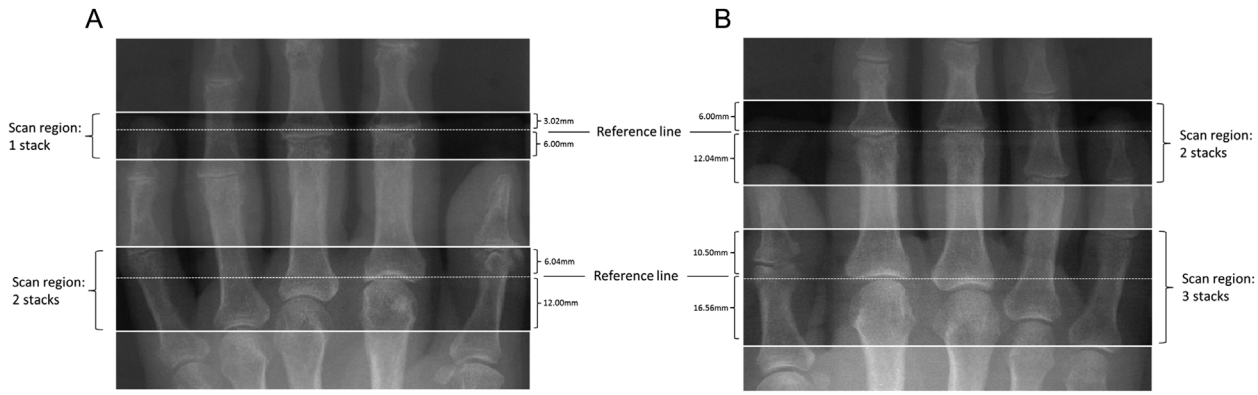

Fig. 1. Scout views of a left (*A*) and right (*B*) hand, showing the regions that were scanned by a greater volume of peripheral quantitative computed tomography scans of the metacarpophalangeal (MCP) and proximal interphalangeal (PIP) joints following the first (*A*) and second (*B*) scan protocols. The top of the MCP head and PIP of the most distal joint (MCP2 and PIP2 in *A*, and MCP2 and PIP3 in *B*) were chosen as the landmarks for the placement of the reference line. It can be seen that with both scan protocols the total joint is encapsulated in the scan region. Thus, the total region where cortical interruptions can occur is included with both scan protocols.

Image analyses

The outer margin of the cortex was identified using an autocontouring algorithm.[29] The contours were visually inspected and, if necessary, adjusted by an operator. A segmentation to distinguish bone and nonbone was performed using the standard evaluation protocol from the manufacturer, which included Laplace-Hamming filtering and thresholding.[35]

Cortical interruptions

An automated algorithm for the detection of cortical interruptions and underlying trabecular bone void was applied to all binary images and is described in previous work.[29–31] In short, first, a cortical mask with a constant depth of 4 voxels (0.328 mm) was generated based on the outer contour. Second, the bone within this mask was analyzed for cortical interruptions with a diameter of $\geq$0.41 mm.[30] Third, a region of interest (ROI) of approximately 4 mm around these cortical interruptions was identified for MCP joints and 2 mm for PIP joints.[31] Fourth, voids in this ROI $\geq$0.41 mm in radius were selected; only those connected to the cortical interruptions were included as underlying trabecular voids.[31]

Per joint, a number of cortical interruptions, an interruption surface area, and an interruption volume (cortical interruption and trabecular void volume) were obtained (ie, cortical interruption parameters). In addition, the proportion of joints with at least two cortical interruptions (proportion of joints affected) was calculated. This cut-off value was chosen because we expected at least one physiological interruption in the joints because of the presence of vascular channels.[36]

Bone density and microstructure parameters

The standard and cortical evaluation protocols were used to determine the volumetric bone density and microstructure parameters as described elsewhere.[26,37] The vBMD (mgHA/cm^3) was calculated for the total (Tot.BMD), trabecular (Tb.BMD), and cortical (Ct.BMD) regions. Additionally, the density of the cortical bone tissue was measured (Ct.TMD). Furthermore, Tb.N (mm^{-1}), thickness (μm), and separation (Tb.Sp; μm), as well as the intraindividual distribution of separation (Tb.SpSD; μm) were determined to assess the trabecular compartment. The cortical thickness (Ct.Th; μm), cortical porosity (Ct.Po; %), and cortical pore diameter (Ct.Po.Dm; μm) were determined to assess the cortical compartment.

CR acquisition and scoring

Posteroanterior radiographs of the hands were taken of all subjects according to a standard clinical protocol. Two experienced and trained rheumatologists, who were blinded for clinical data, independently scored the radiographs of the hands to assess structural bone damage according to the Sharp/Van der Heijde (SvdH) method.[38] Agreement between the readers for the SvdH hand score was excellent, with an intraclass correlation coefficient (ICC) = 0.96 (95% CI, 0.93 to 0.97). Mean scores of the two readers were calculated and used for the analysis.

We additionally examined the SvdH erosion scores on the second and third MCP and PIP joints (radiographic damage). Radiographic damage was defined as the SvdH erosion score of the specific joint.

MRI acquisition and scoring

The second and third MCP and PIP joints of both hands were examined using a 3.0-T Achieva Philips (Philips, Andover, MA, USA) MRI device. During the examination, the hand was fixed inside a dedicated wrist coil, and the space around the hand was filled with rubber to reduce motion artifacts. Images were acquired of both hands using axial T1-weighted, axial fat-suppressed T2-weighted, and sagittal 3D WATSc (water-selective cartilage scan) sequences. Additional images were acquired postintravenous gadolinium (Gadovist 1.0 mmol/mL solution for injection; Schering AG, Berlin, Germany) using axial and coronal fat-suppressed T1-weighted images.

The MR images were independently scored by two radiologists (DL and RW), who were blinded for clinical data. The presence

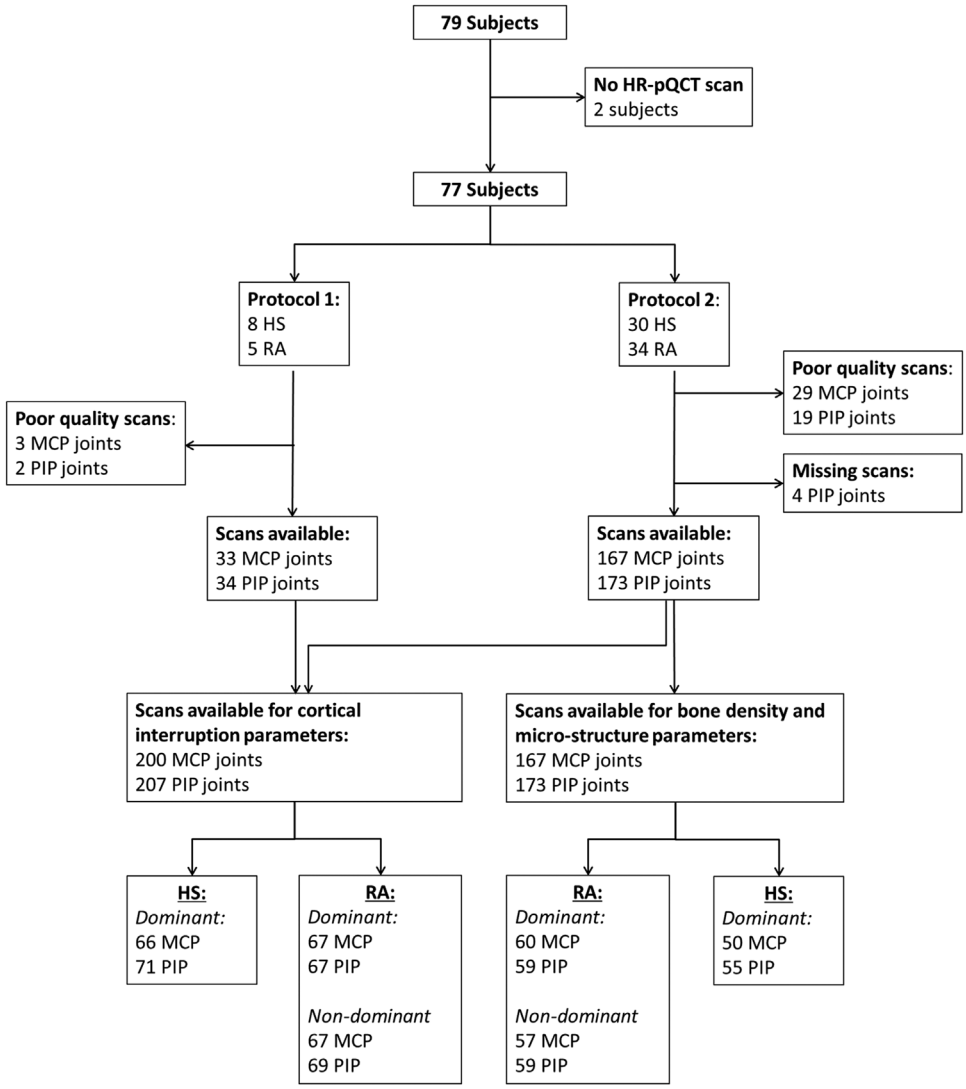

Fig. 2. Schematic overview of the HR-pQCT scans in all subjects, including the number of excluded scans because of poor quality. Both scan protocols are used for analyses of the cortical interruption parameters, but only scan protocol 2 is used for analyses of the bone density and microstructure parameters. HR-pQCT = high-resolution peripheral quantitative computed tomography; HS = healthy subject; MCP = metacarpophalangeal joint; PIP = proximal interphalangeal joint; RA = rheumatoid arthritis.

of erosions was evaluated per joint quadrant per bone end (thus a maximum of eight erosions per joint could be obtained). Synovitis and BME were evaluated per joint (yes/no). Agreement per joint between the readers was good with ICC = 0.75 (95% CI, 0.70 to 0.80) for the number of erosions, and $\kappa = 0.71$ and 0.87 for the presence of synovitis and BME, respectively. Consensus was reached in case of discrepancies.

Statistics

Descriptives per joint were calculated in patients with RA and healthy subjects for the proportion of joints affected, the cortical interruption, bone density, and microstructure parameters on HR-pQCT, and for findings on CR and MRI. Stratified analyses were performed in patients with RA for hand dominance (dominant versus nondominant) and disease duration (early [<2 years] versus longstanding [>2 years]). Differences were tested with independent *t* tests, paired *t* tests, Mann-Whitney *U* tests, or χ^2 tests, as appropriate.

Possible associations were tested: (1) between either structural damage on CR or structural damage and inflammatory markers on MRI, and cortical interruption parameters on HR-pQCT; (2) between the presence of RA and cortical interruption parameters on HR-pQCT; and (3) between either bone density or microstructure parameters and cortical interruption parameters on HR-pQCT. Associations were calculated using repeated-measures generalized estimating equations (GEE) with a negative binomial distribution because of count data (non-normally distributed data) with overdispersion. A repeated exchangeable or unstructured working correlation structure was assumed (which fitted best) to adjust for within-subject correlation. All GEE analyses were performed with data from the dominant hand of each subject and were adjusted for joint (MCP or PIP), digit (second or third digit), age (years), and subject

Table 1. Characteristics of the Participants

	Healthy subjects $n = 38$	Patients with RA $n = 39$	p value
Age, years	51.2 (10.3)	54.8 (7.0)	0.081
Disease duration, months	n/a	131.7 (116.5)	–
ACPA positive	n/a	30 (77%)	
RF positive	n/a	24 (59%)	
ACPA and RF positive	n/a	21 (54%)	
Use of DMARDs	n/a	34 (87%)	–
Use of biologicals	n/a	20 (51%)	–
Use of DMARDs and biologicals	n/a	15 (38%)	–
Smoking			0.624
No	22 (58%)	19 (49%)	
Former	11 (29%)	12 (31%)	
Current	5 (13%)	8 (21%)	

All values are presented as mean (SD) or absolute number (%).In two patients, ACPA values were missing.

RA = rheumatoid arthritis; RF = rheumatoid factor; ACPA = anti-citrullinated protein antibody; DMARD = disease-modifying antirheumatic drug; n/a, not applicable.

(patient with RA or healthy subject), if applicable. In patients with RA, all GEE analyses were repeated using data from both the dominant and nondominant hand with adjustment for hand dominance (dominant or nondominant).

The added value of findings on HR-pQCT over findings on CR or MRI was tested in two additional models (model 2 and model 3) in which the association between the presence of RA and cortical interruption parameters on HR-pQCT was investigated. In model 2, the analysis was additionally adjusted for findings on CR (SvdH hand score and radiographic damage). In model 3, the analysis was additionally adjusted for findings on MRI (number of erosions and presence of synovitis and BME).

Statistical analyses were performed using IBM SPSS Statistics for Windows, Version 20.0 (IBM Corp., Armonk, NY, USA) and SAS software version 9.3 (SAS Institute Inc., Cary, NC, USA).

Results

Two patients with RA did not have HR-pQCT scans available and were excluded from further analyses (Fig. 2). In one patient with RA, HR-pQCT images of the PIP joints were missing because of an intolerance to long immobilization during scanning, but the remaining joints were included in the analyses (Fig. 2). Table 1 shows the characteristics of the study population. Patients with RA tended to be older, and their mean (SD) disease duration was 131.7 (116.5) months.

Cortical interruption parameters on HR-pQCT

Table 2 shows that in the MCP joints of patients with RA, significantly more cortical interruptions were detected and in more joints, compared with healthy subjects. In addition, a significantly larger surface area and a greater volume of cortical interruptions per joint in patients with RA compared with healthy subjects were found.

For MCP joints, comparative stratified analyses in patients with RA showed a significantly greater interruption volume in patients with longstanding RA compared with early RA patients.

Table 2. Values of the HR-pQCT Cortical Interruption Parameters in MCP and PIP Joints in Healthy Subjects and Patients With RA

				Patients with RA					
	Healthy subjects $n = 66$	Patients with RA $n = 134$	p value	Nondominant t $n = 59$[a]	Dominant hand $n = 59$[a]	p value	Early RA $n = 39$	Longstanding RA $n = 95$	p value
MCP joints									
Joints affected (%)	39.4	58.2	0.012	50.9	64.4	0.136	51.3	61.1	0.298
Number of interruptions	1.00 (0–2.25)	2.00 (1.00–5.25)	<0.001	2.00 (1.00–4.00)	2.00 (1.00–7.00)	0.022	2.00 (1.00–3.00)	2.00 (1.0–6.00)	0.133
Interruption surface area (mm^2)	0.69 (0–1.79)	1.42 (0.55–6.24)	0.001	1.18 (0.29–3.85)	1.47 (0.76–13.51)	0.022	0.99 (0.55–1.89)	1.63 (0.54–16.06)	0.058
Interruption volume (mm^3)	0.23 (0–0.68)	0.48 (0.18–8.56)	<	0.39 (0.10–2.82)	0.56 (0.25–37.51)	0.005	0.32 (0.18–0.68)	0.73 (0.18–32.22)	0.031
PIP joints	$n = 71$	$n = 136$		$n = 64$[a]	$n = 64$[a]		$n = 40$	$n = 96$	
Joints affected(%)	15.5	30.2	0.021	26.6	34.4	0.337	20.0	34.4	0.096
Number of interruptions	0 (0–1.00)	1.00 (0–2.00)	0.123	1.00 (0–2.00)	1.00 (0–2.75)	0.011	0 (0–1.00)	1.00 (0–2.00)	0.102
Interruption surface area (mm^2)	0 (0–1.10)	0.42 (0–2.00)	0.217	0.29 (0–1.87)	0.64 (0–2.66)	0.135	0 (0–1.23)	0.57 (0–2.66)	0.100
Interruption volume (mm^3)	0 (0–0.55)	0.14 (0–0.94)	0.283	0.10 (0–0.61)	0.21 (0–1.56)	0.119	0 (0–0.40)	0.19 (0–1.35)	0.092

Values are displayed as percentage or median (IQR).

RA = rheumatoid arthritis; IQR = interquartile range; Joints affected = joints with at least two interruptions; early RA = RA <2-year disease duration; longstanding RA = RA >2-year disease duration; MCP = metacarpophalangeal; PIP = proximal interphalangeal joint; HR-pQCT = high-resolution peripheral quantitative computed tomography.

[a]Joints were included only if both the dominant and nondominant scans were available.

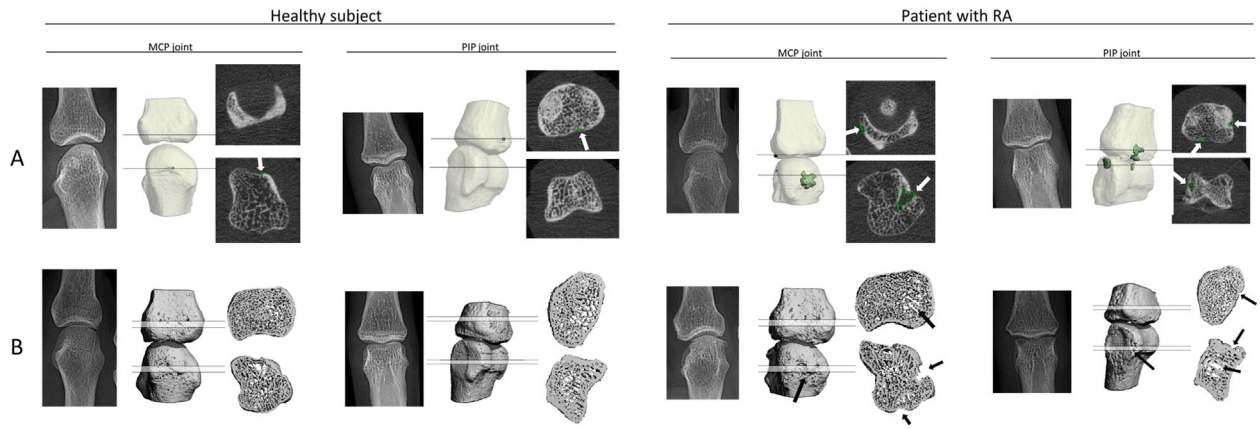

Fig. 3. Typical examples of metacarpophalangeal and proximal interphalangeal joints in patients with rheumatoid arthritis and healthy subjects with no structural damage on CR. (*A*) Cortical interruptions (green) detected in 3D and the corresponding 2D slices are shown. Cortical interruptions were found in both patients with RA and healthy subjects, but more and larger interruptions were detected in the patients with RA. (*B*) The 3D bone microstructure and 10-slice-thick corresponding axial slices are shown; the arrows indicate where there is an absence of trabecular and/or cortical structure in patients with RA as compared with healthy subjects. RA = rheumatoid arthritis; MCP = metacarpophalangeal; PIP = proximal interphalangeal.

Furthermore, in the dominant hand of patients with RA, significantly more cortical interruptions and a larger surface area, as well as a greater volume of interruptions could be detected compared with the nondominant hand.

For PIP joints, similar but smaller differences were found between patients with RA and healthy subjects, and in the stratified analyses in patients with RA. Statistical significance was only found for the proportion of joints affected between patients with RA and healthy subjects, and for the number of interruptions in the dominant versus the nondominant hand.

Figure 3*A* shows examples of cortical interruptions detected in the MCP and PIP joints of a healthy subject and a patient with RA.

Findings on CR and MRI

Seventy-five baseline radiographs of the 77 subjects with an HR-pQCT scan were available and scored (39 patients with RA and 36 healthy subjects). The mean SvdH score based on two readers was significantly higher in patients with RA versus healthy subjects (mean = 9.1; SD = 17.3; range, 0 to 87.5) versus 1.1 (SD = 1.8; range, 0 to 10; $p = 0.008$). In 10 joints from five patients with RA, radiographic damage was present in the joints specifically examined with HR-pQCT and MRI (MCP2, 3 and PIP 2, 3). In healthy subjects, no radiographic damage was observed in these joints.

Seventy-five baseline MRI scans of the 77 subjects who received an HR-pQCT scan were available and scored (38 patients with RA and 37 healthy subjects). In one subject, images of four PIP joints were missing because of technical issues. Based on motion artifacts found on MRI, 12 joints were not evaluable for BME and 14 joints were not evaluable for erosion and synovitis. In patients with RA, significantly more joints with erosions, BME, and synovitis were found compared with healthy subjects (Table S1). Longstanding RA patients had a significantly higher proportion of joints with BME compared with early RA patients. Furthermore, the mean number of erosions was significantly higher in the dominant hand compared with the nondominant hand in patients with RA (Table S1).

Associations between findings on CR or MRI with the cortical interruption parameters on HR-pQCT

Table 3 presents the results of our GEE analysis investigating associations between findings on either CR or MRI and cortical interruption parameters. Radiographic damage in the joint and the SvdH hand score on CR were significantly associated with more cortical interruptions and both a larger surface area and a greater volume of cortical interruptions per joint on HR-pQCT (prevalence ratios [PRs] ranging from 1.03 to 2.04; all $p < 0.01$).

Also, the presence and number of erosions, BME, and synovitis per joint on MRI were each significantly associated with more cortical interruptions and both a larger surface area and a greater volume of cortical interruptions per joint on HR-pQCT (PRs ranging from 1.32 to 7.74; all $p < 0.01$; Table 3).

Similar associations were found in additional analyses using data from both the dominant and nondominant hand of patients with RA (Table S2).

Added value of HR-pQCT over CR or MRI

The association between the presence of RA and each of the cortical interruption parameters was tested in a model with adjustment for joint, digit, and age. Significant associations were found, with PRs ranging from 2.33 to 5.39 (Table 4, model 1).

The added value of HR-pQCT over findings on CR or MRI was tested in two additional models. After adjustment for structural damage on CR (Table 4, model 2) or structural damage and inflammatory markers on MRI (Table 4, model 3), still significant associations between the presence of RA and cortical interruptions parameters were found, indicating that the HR-pQCT has an added value over findings on CR and MRI in the detection of cortical interruptions and in the distinction between patients with RA and healthy subjects.

Figure 3*A* shows examples of cortical interruptions detected on HR-pQCT in MCP and PIP joints of a patient with RA and a healthy subject with no structural damage on CR. It can be seen that more and larger interruptions are detected in the patient with RA versus the healthy subject, despite no visible structural damage on CR in both subjects.

Table 3. Associations Between Structural Damage on CR and Structural Damage and Inflammatory Features on MRI, and Bone Density Parameters on HR-pQCT With the Cortical Interruption parameters on HR-pQCT

	Number of interruptions			Interruption surface area			Interruption volume		
	β	PR (95% CI)	*p* value	β	PR 95% CI)	*p* value	β	PR (95% CI)	*p* value
CR									
SvdH hand score	0.03	1.03 (1.02–1.05)	<0.001	0.06	1.07 (1.04–1.09)	<0.001	0.08	1.08 (1.05–1.11)	<0.001
Radiographic damage	0.33	1.40 (1.14–1.70)	0.001	0.55	1.74 (1.18–2.56)	0.005	0.71	2.04 (1.19–3.49)	0.010
MRI									
Erosion (presence)	0.75	2.12 (1.53–2.94)	<0.001	1.76	5.79 (3.26–10.30)	<0.001	2.01	7.47 (3.41–16.39)	<0.001
Number of erosions	0.28	1.32 (1.21–1.45)	<0.001	0.61	1.84 (1.52–2.24)	<0.001	0.65	1.92 (1.44–2.56)	<0.001
BME (presence)	0.83	2.29 (1.42–3.68)	<0.001	1.78	5.91 (2.52–13.87)	<0.001	1.90	6.68 (1.96–22.76)	0.002
Synovitis (presence)	1.35	3.84 (2.58–5.74)	<0.001	2.04	7.71 (3.48–17.06)	<0.001	2.05	7.74 (2.45–24.49)	<0.001
HR-pQCT									
Tot.BMD[a]	−0.06	0.94 (0.91–0.98)	0.001	−0.08	0.92 (0.87–0.98)	0.008	−0.09	0.91 (0.86–0.98)	0.008
Tb.BMD[a]	−0.05	0.95 (0.89–1.02)	0.144	−0.06	0.94 (0.84–1.06)	0.303	−0.15	0.87 (0.76–0.99)	0.029
Ct.BMD[a]	−0.09	0.91 (0.88–0.95)	<0.001	−0.18	0.84 (0.79–0.89)	<0.001	−0.13	0.88 (0.81–0.96)	0.005
Ct.TMD[a]	−0.09	0.91 (0.88–0.95)	<0.001	−0.20	0.82 (0.77–0.87)	<0.001	−0.17	0.84 (0.77–0.93)	<0.001

Analyses were performed with data from the dominant hand of each subject. Values displayed as value or value (95% CI). Models adjusted for joint, digit, age, and RA.

PR = prevalence ratio; BMD = bone mineral density; Tot.BMD = total volumetric BMD; Tb.BMD = trabecular volumetric BMD; Ct.BMD = cortical volumetric BMD; Ct.TMD = cortical volumetric tissue mineral density; MRI = magnetic resonance imaging; BME = bone marrow edema; CR = conventional radiography; SvdH hand score = Sharp/Van der Heijde hand score; radiographic damage = SvdH erosion score in specific MCP or PIP joint; HR-pQCT = high-resolution peripheral quantitative computed tomography.

[a]β and PR values are displayed per 10 unit increase.

Bone density and microstructure parameters

In both MCP and PIP joints, we found that the vBMD was lower in patients with RA compared with healthy subjects in the total, trabecular, and cortical regions (Tables S3, S4). Moreover, the mineralization of the Ct.TMD was lower in patients with RA than in healthy subjects. Furthermore, the Tb.N was lower and the Tb.Sp higher with more variance in the distribution of separation (Tb.SpSD higher). In addition, a thinner Ct.Th (lower) and smaller Ct.Po.Dm (lower) were observed in patients with RA compared with healthy subjects (Tables S3, S4).

Comparative stratified analyses showed that in patients with longstanding RA compared with early RA, significantly thinner trabeculae in MCP joints were found.

Figure 3*B* shows examples of trabecular and cortical bone loss in the MCP and PIP joints of the dominant hand in a patient with RA versus that of a healthy subject.

Associations between bone density or microstructure with the cortical interruption parameters

A significant negative association was found between the vBMD parameters and the cortical interruption parameters per joint, except for the association between Tb.BMD and the number and surface area of interruptions (PRs ranging from 0.82 to 0.95 per 10 unit vBMD increase; Table 3).

The bone microstructure parameters did not show any significant associations with the cortical interruption parameters per joint, except for Tb.N and Tb.Sp with interruption volume (PRs: 0.21; 95% CI, 0.05 to 0.83; and 22.89; 95% CI, 1.67 to 313.75, respectively).

Similar associations were found in additional analyses using data from both the dominant and nondominant hands of patients with RA (Table S2).

Discussion

The present study showed that more and larger cortical interruptions were found on HR-pQCT in patients with RA than in healthy subjects. These differences were primarily found in MCP joints and not in PIP joints, as expected.[39] More and larger interruptions were found in longstanding RA patients versus early RA patients, but the difference was only significant for the interruption volume in MCP joints. Structural damage observed on CR and MRI and markers of inflammation (BME and synovitis) on MRI were significantly associated with more cortical interruptions and both a larger surface area and a

Table 4. Associations Between the Presence of RA and Each of the Cortical Interruption Parameters on HR-pQCT

		Number of interruptions			Interruption surface area			Interruption volume		
		β	PR (95% CI)	*p* value	β	PR (95% CI)	*p* value	β	PR (95% CI)	*p* value
RA	Model 1	0.84	2.33 (1.50–3.60)	<0.001	1.42	4.14 (2.21–7.73)	<0.001	1.68	5.39 (2.66–10.92)	<0.001
	Model 2	0.57	1.77 (1.14–2.75)	0.011	0.81	2.25 (1.29–3.94)	0.004	0.95	2.59 (1.25–5.36)	0.011
	Model 3	0.52	1.68 (1.10–2.57)	0.017	0.67	1.95 (1.08–3.53)	0.027	1.03	2.80 (1.17–6.71)	0.021

Analyses were performed with data from the dominant hand of each subject. Values displayed as value or value (95% CI).

Model 1: adjustment for joint, digit, and age; Model 2: adjustment for joint, digit, age, radiographic damage, and SvdH hand score on CR; Model 3: adjustment for joint, digit, age, erosions, BME, and synovitis on MRI.

RA = rheumatoid arthritis; PR = prevalence ratio; SvdH score = Sharp/van der Heijde score; CR = conventional radiography; MRI = magnetic resonance imaging; BME = bone marrow edema; radiographic damage = SvdH erosion score in specific metacarpophalangeal or proximal interphalangeal joint.

greater volume of cortical interruptions on HR-pQCT. In addition, the presence of RA was significantly associated with the number, surface area, and volume of cortical interruptions on HR-pQCT, even after adjustment for findings on CR and MRI, indicating an added value of the HR-pQCT. Moreover, bone density and microstructural parameters were impaired in patients with RA, and a lower bone density was associated with more interruptions and both a larger surface area and a greater volume of interruptions on HR-pQCT. For example, every erosion on MRI was associated with a 1.32 times (32%) increase of the number of interruptions, a 1.84 times (84%) increase of interruption surface area, and a 1.92 times (92%) increase of interruption volume.

In the present study, we found, on average, a higher number of cortical interruptions in MCP joints of patients with RA than has been reported in previous studies, which used visual scoring of HR-pQCT images (mean number of cortical interruptions was 4.3 in our study versus means ranging from 0.7 to 3.0 in previous studies).[15–18,40,41] This suggests that we indeed included smaller-sized interruptions with our semiautomated algorithm compared with visual scoring of interruptions on HR-pQCT.

Our observation that more small cortical interruptions could be detected on HR-pQCT in patients with RA as opposed to healthy subjects is in line with a previous study.[24] In that study, using visual scoring on binary images, more very small cortical interruptions (with a diameter $\geq$0.082 mm) were found in patients with RA versus healthy subjects (112.9 versus 75.2).[24] Small interruptions might serve as a starting point for pathological cortical interruptions.[42] Monitoring these individual small cortical interruptions might be useful in understanding the pathogenesis of RA and might also be of value for evaluating the progression of structural damage or responsiveness to treatment in individual patients with RA. Previous research demonstrated, for example, repair processes of existing large pathological interruptions with HR-pQCT in those patients using tumor necrosis factor inhibitors, interleukin-6, or receptor activator of nuclear factor kappa B ligand (RANKL) blockers.[15,16,43]

We also found associations between the dominant hand (versus the nondominant hand), the MCP joint (versus the PIP joint), digit 2 (versus digit 3), a higher age, a lower vBMD, and more and larger interruptions in finger joints on HR-pQCT. In studies using CR, higher SvdH scores have been reported for the dominant hand versus the nondominant hand.[44,45] More and larger interruptions in the dominant hand support the hypothesis that mechanical factors also play a role in the development of erosions.[1,5] Using HR-pQCT, Stach and colleagues showed that most interruptions could be found in the second MCP joint.[11] Werner et al. showed that the number of small cortical interruptions in finger joints on HR-pQCT increases with increasing age.[24] Last, Rossini and colleagues showed that a lower BMD in the hip or spine measured on DXA was correlated with more interruptions on CR.[46]

Another observation in the present study was that the bone density and microstructural parameters were impaired in patients with RA in contrast to healthy subjects. A lower bone density in both the trabecular and cortical regions, fewer trabeculae (Tb.N lower, Tb.Sp and Tb.SpSD higher), and a thinner cortex were found in patients with RA. This is in agreement with previous studies investigating bone density and microstructure parameters in patients with RA compared with healthy subjects using HR-pQCT,[14,47] although the study from Fouque-Aubert and colleagues reported thinner trabeculae rather than fewer trabeculae as was found in our study.[14] This difference might be explained by the longer scan region in our study than in the study of Fouque-Aubert and colleagues (three stacks, 27.06 mm versus one stack, 9.02 mm), because fewer trabeculae are present more distally from the joint.[14] In addition to the standard evaluation protocol, we were the first to apply the cortical evaluation protocol, which also evaluates the cortical-tissue mineral density and porosity in finger joints of patients with RA as opposed to healthy subjects. The cortical tissue mineral density was significantly lower in patients with RA, meaning that the decrease in Ct.BMD is not only caused by the loss of cortical bone, but also by a decrease in the density of cortical bone tissue. Interestingly, in both MCP and PIP joints, the Ct.Po and Ct.Po.Dm were smaller in patients with RA than in healthy subjects. This might seem contraintuitive, but it should be noted that these Ct.Po measurements only involve intracortical pores—hence cortical interruptions are excluded. Because the cortical porosity and cortical pore parameter only involve intracortical pores, expanded intracortical pores are likely to become cortical interruptions, and thus are not included in these parameters. Hence, this might lead to a decrease in the Ct.Po and Ct.Po.Dm and an increase in the cortical interruption parameters in patients with RA.

Our study has several limitations. First, we did not visually inspect and correct the inner cortical contour for determination of the cortical density and cortical microstructural parameters. However, in a separate study of the MCP joints in early arthritis patients, a high reproducibility on scan/rescan data with in-between repositioning of these parameters without correcting the inner cortical contour was found, indicating that the determination of the inner cortical contour was reliable, and only slightly dependent on repositioning and motion artifacts.[31] Second, with our algorithm, the trabecular void volume underlying the cortical interruption that can be detected is limited to a depth of 4 mm in MCP joints and 2 mm in PIP joints. This means that the algorithm underestimates the volume of interruptions with a depth greater than these cut-offs (ie, volume $>$134 mm^3 and $>$16.8 mm^3, respectively). Hence, the comparability of the 3D volume of very large interruptions may be limited between our algorithm and other techniques. However, such large interruptions are not the primary focus of research with HR-pQCT because these can also be detected by other imaging techniques with lower resolution (eg, CR and MRI). The strength of HR-pQCT lies mainly in the detection of "small" interruptions, $<$10 mm^3, which are missed with MRI.[48] Third, our study was performed using the first-generation HR-pQCT. Meanwhile, the second-generation HR-pQCT (HR-pQCT2) has been introduced, which has a higher spatial resolution (95 μm versus 130 μm) and smaller voxel size (61 μm versus 82 μm). This higher resolution enables better distinction between bone and nonbone, which may reduce the number of falsely detected interruptions due to the partial volume effect.[29] Additionally, the minimum interruption diameter will be smaller when applying two dilation steps ($\geq$0.305 mm versus $\geq$0.410 mm, respectively). The detection of more and smaller cortical interruptions with a possible higher validity of these interruptions may both increase the added value of HR-pQCT over findings on MRI and CR in the detection of cortical interruptions and in the distinction of patients with RA from healthy subjects.

The present study has shown that our algorithm is able to detect these small cortical interruptions and showed differences in patients with RA and healthy subjects beyond structural damage on CR, and structural damage and inflammatory markers on MRI. Only small differences between early RA and

longstanding RA patients were found. This may indicate that the patients were treated effectively (51% of the patients are treated with biologicals). The algorithm can best be used in arthritis patients aiming at early detection of structural damage. The next step is to apply this algorithm in a clinical follow-up study to test its potential value in monitoring patients with RA.

In conclusion, using our semiautomated algorithm, we demonstrated a higher number of interruptions, and both a larger surface area and volume of interruptions on HR-pQCT in early and longstanding RA patients than in healthy subjects. Structural damage on CR and MRI and markers of inflammation (BME and synovitis) on MRI were associated with these cortical interruption parameters on HR-pQCT. HR-pQCT has shown to be of added value over findings on CR and MRI in the detection of cortical interruptions and in the distinction of patients with RA versus healthy subjects. We also found impaired bone density and microstructure in patients with RA compared with healthy subjects, and that lower bone density was associated with more and larger interruptions on HR-pQCT. These findings demonstrate the value of HR-pQCT imaging in the evaluation of periarticular bone and in the assessment of (early) bone damage in addition to CR and MRI in patients with RA.

Disclosures

PG received grants from AMGEN, ABBVIE, MSD, WILL, ROCHE, BMS, and UCB S.A. BvR is a consultant for Scanco Medical AG, Bruettisellen, Switzerland.

Acknowledgments

The work was supported by unrestricted grants from the Weijerhorst Foundation (WH-2) and Pfizer (WS2056904). We thank Dr. D. Vosse and Dr. T. Schoonbrood, rheumatologists at the Maastricht University Medical Center, for scoring of the conventional radiographs.

Authors' roles: MP: study design, data collection, analyses, interpretation of data, drafting the article, final approval; AvT, PG, JvdB, BvR: study design, interpretation of data, critical revision of the article, final approval; JD: analyses, interpretation of data, final approval; AS, DL, RW: data collection, critical revision of the article, final approval.

References

1. Schett G, Gravallese E. Bone erosion in rheumatoid arthritis: mechanisms, diagnosis and treatment. Nat Rev Rheumatol. 2012 Nov;8(11):656–64.
2. Geusens P, van den Bergh J. Bone erosions in rheumatoid arthritis. Rheumatology. 2014 Jan;53(1):4–5.
3. Ejbjerg B, Narvestad E, Rostrup E, et al. Magnetic resonance imaging of wrist and finger joints in healthy subjects occasionally shows changes resembling erosions and synovitis as seen in rheumatoid arthritis. Arthritis Rheum. 2004 Apr;50(4):1097–106.
4. Baillet A, Gaujoux-Viala C, Mouterde G, et al. Comparison of the efficacy of sonography, magnetic resonance imaging and conventional radiography for the detection of bone erosions in rheumatoid arthritis patients: a systematic review and meta-analysis. Rheumatology. 2011 Jun;50(6):1137–47.
5. Geusens P, Chapurlat R, Schett G, et al. High-resolution in vivo imaging of bone and joints: a window to microarchitecture. Nat Rev Rheumatol. 2014 May;10(5):304–13.
6. Dohn UM, Ejbjerg BJ, Hasselquist M, et al. Detection of bone erosions in rheumatoid arthritis wrist joints with magnetic resonance imaging, computed tomography and radiography. Arthritis Res Ther. 2008; 10(1):R25.
7. Dohn UM, Ejbjerg B, Boonen A, et al. No overall progression and occasional repair of erosions despite persistent inflammation in adalimumab-treated rheumatoid arthritis patients: results from a longitudinal comparative MRI, ultrasonography, CT and radiography study. Ann Rheum Dis. 2011 Feb;70(2):252–8.
8. Gandjbakhch F, Foltz V, Mallet A, Bourgeois P, Fautrel B. Bone marrow oedema predicts structural progression in a 1-year follow-up of 85 patients with RA in remission or with low disease activity with low-field MRI. Ann Rheum Dis. 2011 Dec;70(12):2159–62. Epub 2011 Aug 24.
9. Hetland ML, Ejbjerg B, Horslev-Petersen K, et al. MRI bone oedema is the strongest predictor of subsequent radiographic progression in early rheumatoid arthritis. Results from a 2-year randomised controlled trial (CIMESTRA). Ann Rheum Dis. 2009 Mar;68(3):384–90.
10. Peterfy C, Strand V, Tian L, et al. Short-term changes on MRI predict long-term changes on radiography in rheumatoid arthritis: an analysis by an OMERACT Task Force of pooled data from four randomised controlled trials. Ann Rheum Dis. 2017 Jun;76(6):992–7.
11. Stach CM, Bauerle M, Englbrecht M, et al. Periarticular bone structure in rheumatoid arthritis patients and healthy individuals assessed by high-resolution computed tomography. Arthritis Rheum. 2010 Feb;62(2):330–9.
12. Regensburger A, Rech J, Englbrecht M, et al. A comparative analysis of magnetic resonance imaging and high-resolution peripheral quantitative computed tomography of the hand for the detection of erosion repair in rheumatoid arthritis. Rheumatology (Oxford). 2015 Sep;54(9):1573–81. Epub 2015 Apr 3.
13. Lee CH, Srikhum W, Burghardt AJ, et al. Correlation of structural abnormalities of the wrist and metacarpophalangeal joints evaluated by high-resolution peripheral quantitative computed tomography, 3 Tesla magnetic resonance imaging and conventional radiographs in rheumatoid arthritis. Int J Rheum Dis. 2015 Jul;18-(6):628–39. Epub 2014 Oct 9.
14. Fouque-Aubert A, Boutroy S, Marotte H, et al. Assessment of hand bone loss in rheumatoid arthritis by high-resolution peripheral quantitative CT. Ann Rheum Dis. 2010 Sep;69(9):1671–6.
15. Finzel S, Rech J, Schmidt S, et al. Repair of bone erosions in rheumatoid arthritis treated with tumour necrosis factor inhibitors is based on bone apposition at the base of the erosion. Ann Rheum Dis. 2011 Sep;70(9):1587–93.
16. Finzel S, Rech J, Schmidt S, Engelke K, Englbrecht M, Schett G. Interleukin-6 receptor blockade induces limited repair of bone erosions in rheumatoid arthritis: a micro CT study. Ann Rheum Dis. 2013 Mar;72(3):396–400.
17. Srikhum W, Virayavanich W, Burghardt AJ, et al. Quantitative and semiquantitative bone erosion assessment on high-resolution peripheral quantitative computed tomography in rheumatoid arthritis. J Rheum. 2013 Apr;40(4):408–16.
18. Topfer D, Finzel S, Museyko O, Schett G, Engelke K. Segmentation and quantification of bone erosions in high-resolution peripheral quantitative computed tomography datasets of the metacarpophalangeal joints of patients with rheumatoid arthritis. Rheumatology. 2014 Jan;53(1):65–71.
19. Topfer D, Gerner B, Finzel S, et al. Automated three-dimensional registration of high-resolution peripheral quantitative computed tomography data to quantify size and shape changes of arthritic bone erosions. Rheumatology. 2015 Dec;54(12):2171–80. 2015 Jul 14.
20. Barnabe C, Toepfer D, Marotte H, et al. Definition for rheumatoid arthritis erosions imaged with high resolution peripheral quantitative computed tomography and interreader reliability for detection and measurement. J Rheum. 2016 Oct;43(10):1935–40.
21. Scharmga A, Peters M, van Tubergen A, et al. Heterogeneity of cortical breaks in hand joints of patients with rheumatoid arthritis and healthy controls imaged by high-resolution peripheral quantitative computed tomography. J Rheum. 2016 Oct;43(10): 1914–20.
22. Binks DA, Gravallese EM, Bergin D, et al. Role of vascular channels as a novel mechanism for subchondral bone damage at cruciate

ligament entheses in osteoarthritis and inflammatory arthritis. Ann Rheum Dis. 2015 Jan;74(1):196–203.

23. Schett G, Stolina M, Bolon B, et al. Analysis of the kinetics of osteoclastogenesis in arthritic rats. Arthritis Rheum. 2005 Oct;52(10): 3192–201.
24. Werner D, Simon D, Englbrecht M, et al. Rheumatoid arthritis is characterized by early changes of the cortical micro-channel (CoMiC) system in the bare area of the joints. Arthritis Rheum. 2017 Aug;69(8):1580–7.
25. Simon D, Kleyer A, Stemmler F, et al. Age- and sex-dependent changes of intra-articular cortical and trabecular bone structure and the effects of rheumatoid arthritis. J Bone Miner Res. 2017 Apr; 32(4):722–30.
26. Boutroy S, Bouxsein ML, Munoz F, Delmas PD. In vivo assessment of trabecular bone microarchitecture by high-resolution peripheral quantitative computed tomography. J Clin Endocrinol Metab. 2005 Dec;90(12):6508–15.
27. Zebaze R, Seeman E. Cortical bone: a challenging geography. J Bone Miner Res. 2015 Jan;30(1):24–9.
28. Scharmga A, Peters M, van Tubergen A, et al. Visual detection of cortical breaks in hand joints: reliability and validity of high-resolution peripheral quantitative CT compared to microCT. BMC musculoskeletal disorders. 2016;17(1):271.
29. Peters M, Scharmga A, de Jong J, et al. An automated algorithm for the detection of cortical interruptions on high resolution peripheral quantitative computed tomography images of finger joints. PloS One. 2017;12(4):e0175829.
30. Peters M, Scharmga A, van Tubergen A, et al. The reliability of a semi-automated algorithm for detection of cortical interruptions in finger joints on high resolution CT compared to microCT. Calcif Tissue Int. 2017 Aug;101(2):132–40.
31. Peters M, de Jong J, Scharmga A, et al. The reproducibility of a semi-automatic algorithm in the detection of cortical breaks and adjacent trabecular bone loss in scan-rescan data from patients with early arthritis [abstract]. Arthritis Rheum. 2016;68 (suppl 10).
32. Aletaha D, Neogi T, Silman AJ, et al. 2010 Rheumatoid arthritis classification criteria: an American College of Rheumatology/ European League Against Rheumatism collaborative initiative. Arthritis Rheum. 2010 Sep;62(9):2569–81.
33. Barnabe C, Feehan L. High-resolution peripheral quantitative computed tomography imaging protocol for metacarpophalangeal joints in inflammatory arthritis: the SPECTRA collaboration. J Rheumatol. 2012 Jul;39(7):1494–5.
34. Pialat JB, Burghardt AJ, Sode M, Link TM, Majumdar S. Visual grading of motion induced image degradation in high resolution peripheral computed tomography: impact of image quality on measures of bone density and micro-architecture. Bone. 2012 Jan;50(1):111–8.
35. Laib A, Hauselmann HJ, Ruegsegger P. In vivo high resolution 3D-QCT of the human forearm. Technol Health Care. 1998 Dec; 6(5–6):329–37.
36. Scharmga A, Keller KK, Peters M, van Tubergen A, van den Bergh JP, van Rietbergen B, et al. Vascular channels in metacarpophalangeal joints: a comparative histologic and high-resolution imaging study. Scient Rep. 2017 Aug 21;7(1):8966.
37. Burghardt AJ, Buie HR, Laib A, Majumdar S, Boyd SK. Reproducibility of direct quantitative measures of cortical bone microarchitecture of the distal radius and tibia by HR-pQCT. Bone. 2010 Sep;47(3):519–28.
38. van der Heijde D. How to read radiographs according to the Sharp/ van der Heijde method. J Rheumatol. 2000 Jan;27(1):261–3.
39. van der Heijde DM, van Leeuwen MA, van Riel PL, et al. Biannual radiographic assessments of hands and feet in a three-year prospective followup of patients with early rheumatoid arthritis. Arthritis Rheum. 1992 Jan;35(1):26–34.
40. Finzel S, Englbrecht M, Engelke K, Stach C, Schett G. A comparative study of periarticular bone lesions in rheumatoid arthritis and psoriatic arthritis. Ann Rheum Dis. 2011 Jan;70(1):122–7.
41. Barnabe C, Szabo E, Martin L, Boyd SK, Barr SG. Quantification of small joint space width, periarticular bone microstructure and erosions using high-resolution peripheral quantitative computed tomography in rheumatoid arthritis. Clin Exp Rheumatol. 2013 Mar-Apr;31(2):243–50.
42. Schett G, Gravallese E. Bone erosion in rheumatoid arthritis: mechanisms, diagnosis and treatment. Nat Rev Rheumatol. 2012 Nov;8(11):656–64.
43. Yue J, Griffith JF, Xiao F, et al. Repair of bone erosion in rheumatoid arthritis by denosumab: a high-resolution peripheral quantitative computed tomography study. Arthritis Care Res (Hoboken). 2017 Aug;69(8):1156–63.
44. Koh JH, Jung SM, Lee JJ, et al. Radiographic structural damage is worse in the dominant than the non-dominant hand in individuals with early rheumatoid arthritis. PLoS One. 2015;10(8):e0135409.
45. Owsianik WD, Kundi A, Whitehead JN, Kraag GR, Goldsmith C. Radiological articular involvement in the dominant hand in rheumatoid arthritis. Ann Rheum Dis. 1980 Oct;39(5):508–10.
46. Rossini M, Bagnato G, Frediani B, et al. Relationship of focal erosions, bone mineral density, and parathyroid hormone in rheumatoid arthritis. J Rheumatol. 2011 Jun;38(6):997–1002.
47. Yang H, Yu A, Burghardt AJ, et al. Quantitative characterization of metacarpal and radial bone in rheumatoid arthritis using high resolution- peripheral quantitative computed tomography. Int J Rheum Dis. 2017 Mar;20(3):353–62.
48. Albrecht A, Finzel S, Englbrecht M, et al. The structural basis of MRI bone erosions: an assessment by microCT. Ann Rheum Dis. 2013 Aug;72(8):1351–7.